DEUTSCHES ELEKTRONEN-SYNCHROTRON DESY

DESY SR-76/11
June 1976

DESY-Bibliothek
20. JULI 1976

The Application of Synchrotron Radiation to X-Ray Lithography

by

E. Spiller, D. E. Eastman, R. Feder, W. D. Grobman, W. Gudat, and J. Topalian

IBM Thomas J. Watson Research Center
Yorktown Heights, New York 10598

2 HAMBURG 52 · NOTKESTIEG 1

To be sure that your preprints are promptly included in the
HIGH ENERGY PHYSICS INDEX ,
send them to the following address (if possible by air mail) :

DESY
Bibliothek
2 Hamburg 52
Notkestieg 1
Germany

THE APPLICATION OF SYNCHROTRON RADIATION TO X-RAY LITHOGRAPHY

by

E. Spiller, D.E. Eastman, R. Feder, W.D. Grobman, W. Gudat, and J. Topalian

IBM Thomas J. Watson Research Center
Yorktown Heights, New York 10598

ABSTRACT: Synchrotron radiation from the German electron synchrotron DESY in Hamburg has been used for x-ray lithography. Replications of different master patterns (for magnetic bubble devices, fresnel zone plates, etc.) were made using various wavelengths and exposures. High quality lines down to 500 Å wide have been reproduced using very soft x-rays. The sensitivities of x-ray resists have been evaluated over a wide range of exposures. Various critical factors (heating, radiation damage, etc.) involved with x-ray lithography using synchrotron radiation have been studied. General considerations of storage ring sources designed as radiation sources for x-ray lithography are discussed, together with a comparison with x-ray tube sources. The general conclusion is that x-ray lithography using synchrotron radiation offers considerable promise as a process for forming high quality sub-micron images with exposure times as short as a few seconds.

I. Introduction

Electron-beam and x-ray lithography are the two most promising lithographic technologies with demonstrated linewidth resolution capability below 1 μm. To date, x-ray lithography is much less developed than electron-beam lithography but promises several economic and technological advantages. One disadvantage of x-ray lithography is the low efficiency for the generation of soft x-rays from conventional x-ray sources. Due to this low efficiency, the throughput of an x-ray lithographic system is mainly limited by the available x-ray flux, and long exposure times are required for the replication of high resolution patterns. The choice of alignment procedures for x-ray lithography is severely limited by the low brightness of conventional x-ray sources. Electron storage rings and synchrotrons emit a much higher flux of useable collimated x-rays than any other source, thereby allowing short exposure times (on the order of seconds), large throughputs, less critical resist exposure conditions and simplified geometrical conditions for applications requiring registration. Due to the high collimation of synchrotron radiation, the spatial resolution of x-ray lithography with synchrotron radiation is not limited by penumbral blurring, and rather large distances between mask and wafer can be tolerated (about 1 mm for 1 μ linewidth patterns).

Sychrotron radiation is generated by relativistic electrons as they traverse in curved trajectories the strong magnetic fields of bending magnets in storage rings and synchrotrons. In these magnetic sectors, the accelerating electrons emit a broad continuum of radiation, spanning the infrared through the x-ray range, which is highly collimated in the

instantaneous direction of electron motion. Thus, as the electrons traverse the magnetic bending sectors of the storage ring, the collimated radiation sweeps in an arc (similar to a searchlight beam having an hν-dependent angular spread of roughly $\delta\theta \sim 10^{-3}/E(GeV)$ radians, where E is the electron energy and hν is the photon energy), thereby producing a wedge of radiation whose vertical spread is $\delta\theta$ and whose angular spread is the total angular change of direction within the magnetic field. Generally the electron beam is $\sim$1-10mm^2 in cross-sectional area, resulting in both a bright (power per unit area per unit solid angle) and intense source. Spectral characteristics are described in Section II while other features of storage ring sources are described in the appendix.

Various advantages of x-ray lithography using synchrotron radiation have been demonstrated during a brief visit to the DESY 7.5 GeV synchrotron at Hamburg, Germany. This source furnished us with an intense source of radiation throughout the $\sim$100 eV to $\sim$5 keV photon energy range of interest, and was provided with convenient vacuum and sample chamber facilities. Experimental procedures and the various spectra used to expose resists (obtained using different filter and mask combinations) are presented in Section II. Mask replication with synchrotron radiation is described in Section III, including results using very soft x-rays ($\lesssim$ 700 eV), for which high contrast masks can be readily made using e-beam techniques. X-ray resist evaluation is presented in Section IV, while some critical parameters such as wafer heating and radiation damage to x-ray masks are discussed in Section V. A summary of our experimental results and conclusions are given in Section VI. Finally, in Appendix A we describe the general

characteristics of electron storage rings as sources for x-ray lithography, consider the design parameters of a storage ring optimized for use as an x-ray lithography source, and compare storage ring sources with conventional x-ray tube sources.

II. Experiments

A schematic diagram of the mask-substrate configuration involved in x-ray lithography is shown in Fig. 1. In this configuration, the vacant areas present in the absorber layer of the mask permit the resist on the wafer to be exposed by the incident x-ray beams. This exposed resist is then selectively removed using a developer (positive resist), thus replicating the mask pattern in the resist layer.

Figure 2 schematically illustrates the experimental set-up which was used at the Deutsches Elektronen-Synchrotron (DESY) in Hamburg using the synchrotron radiation continuum as a source. At the sample chamber, which is $\sim$ 40m from the source point, the evacuated beam line accepts an angle corresponding to 1 mrad in the horizontal plane. The divergence of the synchrotron radiation in the vertical direction is $\lesssim$ 1 mrad for photon energies $h\nu \gtrsim 50$ eV. The light beam is split into 2 beams by use of a 4° grazing incidence mirror with a Au coating (Fig. 2a). Both beams were used in our experiments, either directly or after passing through an Al or Be window (Fig.2b). Mask/wafer combinations or filters were mounted on two wheels which were driven by remote-controlled motors so as to move samples into the beam position. By keeping one of the possible eight positions open on both wheels we were able to illuminate fourteen different wafers

during one pump-down cycle. A remote-controlled, fast-closing valve served as a beam shutter. With both wheels in the open-position, the intensity of the photon flux could be measured using a calibrated thermopile. Most of the exposures were carried out in high vacuum. Some of the exposures were done with the vacuum chamber back-filled with up to one torr of He to study the effect of exchange gas on heat dissipation in the mask-wafer arrangement.

The DESY synchrotron is a pulsed light source having a repetition frequency of 50 cycles and duty cycle of about 50%. It was operated at an electron energy of 3.5 GeV and an averaged electron current of 8 mA during our visit. Fig. 3a. shows the spectral intensity of sychrotron radiation of DESY at a distance of 37.9 m from the source point on the electron orbit. Figs. 3b. and 3c. display the synchrotron radiation intensity distributions of hypothetical 1.0 GeV and 0.7 GeV storage rings with a current of $\sim$ 100 mA and a bending magnet field of 12 kOe. Such sources will be discussed in more detail in the appendix, where dedicated sources for x-ray lithography are considered.

The smooth spectral intensity distribution of synchrotron light shown in Fig. 3a. is strongly modified by the optical response of the Au mirror surface, the filters and the mylar substrates of the masks. This is included in our calculation of the power absorbed in the resist for various filter-mask combinations. In Fig. 4 the calculated spectral power absorbed[1,2] in x-ray resist (PMMA - polymethyl-methacrylate) is displayed (for several filter materials) in the range 2 to 50 Å. The total power absorbed in the resist is obtained by integrating the area under the curves over the whole spectral range and is given in Table I for various filter combinations for

wavelengths shorter than 100 Å. This range covers most of the radiation active in producing exposures. The curve corresponding to direct exposure (a) shows that a large contribution to the exposure is due to very soft radiation in the range 45 to 30 Å. A comparison with the curves obtained for 0.3 μ (b) and 1 μm (c) thick filters of PMMA shows that most of the soft radiation is absorbed close to the surface of the resist and does not reach the bottom of a thick resist. Exposure with the unfiltered synchrotron light therefore results in non-uniform exposure throughout the resist thickness, i.e. not a simple exponential attenuation. (See also Fig. 12.) The different filter materials can be used for different long wavelength cutoffs, whereas the decrease of the spectrum at the short wavelength is determined by the spectrum of the synchrotron radiation itself. The short wavelength cutoff cannot be changed easily by absorption filters. However, by reflecting the radiation at different glancing angles from mirror surfaces, one can filter out radiation at the short wavelength side of the spectrum.

At DESY one beam line is available which has a gold-coated mirror and a glancing angle of 4° (see Fig. 2a.). Calculated spectra of the absorbed power in PMMA resist exposed in this beamline are presented in Fig. 5. These curves should, however, be used with caution. The published values of the optical constants of gold[3] may not give the correct reflectivity for a gold mirror at small glancing angles, due in part to hydrocarbon deposits on the mirror which may reduce the actual reflectivity. The main effect of the gold mirror for our experiment is to remove the hard radiation below $\lambda \sim 10$ Å, for which some of our masks and objects have only low contrast.

III. Mask Replication with Synchrotron Radiation

Table II summarizes the ranges of all parameters used in the replication of masks. Resist patterns obtained for some of the parameters are shown in Figs. 6 and 7. In Fig. 6 we show patterns obtained for various distances between mask and wafer (see Fig. 1). Due to the good collimation of synchrotron radiation, penumbral blurring is eliminated and the distance between mask and wafer is limited mainly by diffraction. For example, the first diffraction maximum can be recognized in Figs. 6b and 6c. For distances up to 1 mm these diffraction effects would not interfere with subsequent device fabrication steps for 1 μ linewidth devices.

All our masks have a much smaller contrast for the synchrotron radiation from DESY in the direct beam than they have for AlKα radiation. This can be understood using Fig. 4. Curve g. shows that a 0.8 μ thick gold mask, which has a transmission of 0.01 at 8.3 Å, transmits a considerable amount of radiation at shorter wavelengths. The effective transmission of such a mask for the spectrum emitted by DESY operating at 3.5 GeV is 0.16. This lower contrast reduces the dissolution rate ratio between resist exposed through the clear and opaque regions of the mask, resulting in sloping walls in the pattern. We can eliminate sloping walls by using masks with thicker gold plating and higher contrast, or by using very high exposures in PMMA in a regime where the dissolution rate increases very rapidly with exposure.[4,5] The patterns in Fig. 6 have been obtained with PMMA and relatively high exposures. Fig. 7 shows a set of replicas with sloping walls. The exposure in Fig. 7a is just sufficient to give vertical walls if used with a mask of high contrast. However, the mask used has a contrast of

only 6:1 and consequently the replica has sloping walls. The mask in Fig. 7b has a still lower contrast (3:1). In spite of that, a more acceptable replica than in (a) was obtained from this mask by using PMMA and much higher exposures. Fig. 7c is a replica of a mask which has been transferred from the back to the front of a 75 μ thick silicon wafer. Although the mask has a gold thickness of 1.4 μ the effective contrast is very low due to the short wavelength used for this exposure. Fig. 8 shows the effective wavelength ranges for copying the gold mask through a 75 μ thick silicon wafer. The effective contrast of the mask obtained as the ratio of the areas of the two curves in Fig. 8 is 2.3:1.

The effective contrast of all masks can be drastically increased by using softer x-rays. Published values of the absorption coefficient of heavy elements[2] are about a factor ten too high around $\lambda = 50$ Å. New data[3] obtained with synchrotron radiation give a contrast of 20:1 for a mask made of 0.1 μ thick gold. Figs. 9a and 9b show a copy of a Fresnel zone plate made of 0.1 μ thick gold obtained using synchrotron radiation in the 4° beam. Fig. 9c shows details of a diatom copied in the same way. The photographs prove that structures below 0.1 μ size have enough contrast to allow high quality copies if the hard radiation in the beam is eliminated. The spectrum obtained from DESY in the 4° line is a reasonable approximation to that which would be obtained directly from a smaller dedicated source[6].

IV. Evaluation of X-ray Resists

X-ray resists have been exposed to synchrotron radiation for various times in order to obtain the dissolution rate versus exposure curve for

these resists. A 200 mesh copper grid is used as a mask for these experiments; the thickness of the remaining resist and the difference in resist thickness between exposed and unexposed resists is measured for different development times with a white light Michelson interferometer. The slope of the "thickness versus development time" curve gives the dissolution rate of the resist. For most of our experiments we used the full beam from the synchrotron without additional filters. This beam contains a wide spectrum of wavelengths with large variations in the absorption length. Therefore, the top of the resist obtains a very high exposure of predominently soft radiation while the radiation reaching the bottom of the resist is filtered by the resist above and contains only the harder components. The effects of this filtering on the effective exposure is described in Fig. 4 by the curves a,b,c; the values of the effective exposures obtained from these curves for resist thickness of 0,0.3 and 1 μ are given in Table 2. For most of our experiments we used resists with a thickness of 0.4 μ and are able to determine three different dissolution rates from one development, the initial dissolution rate which corresponds to the highest exposure close to the resist surface, the final dissolution rate at the bottom of the resist and an average dissolution rate determined by the total time required to remove all the resist in the exposed region.

Fig. 10 contains dissolution rate data for polymethylmethacrylate (PMMA) for exposures above the values obtained with conventional sources.[4,5] For these high exposures, concentrated methylisobutylketone (MIBK) removes the exposed resist completely in a fraction of a second, therefore, interruption of the development for a measurement of the thickness is not

possible and we have to dilute the developer to obtain lower dissolution rates. Due to the rapid increase of the dissolution rate with exposure, only a small range of exposures is covered by one developer concentration. For the highest point for each concentration, the exposed resist is completely removed in the time necessary to immerse, remove and dry a wafer (few seconds), therefore, these points represent only a lower limit of the dissolution rate and are marked by an arrow in Fig. 10. For exposure times above five minutes, isopropyl alcohol alone removes the resist in a very short time; a residue is observed in the resist exposed for 24 minutes, while the exposed resist becomes insoluable even in concentrated MIBK for a 50 minute exposure. For this exposure PMMA becomes a negative resist in the same way as has been observed for electron beam exposures.[7] The plot in Fig. 10 gives the average dissolution rate for the removal of a 0.4 μ thick layer of resist; an average exposure rate of $35W/cm^3$ is assumed for the lower exposure scale (see Table I).

Experimental resists with a higher sensitivity for x-ray exposures than PMMA are available[8]. Fig. 11 gives the dissolution rates obtained for experimental resist "76/24" baked at 230°C with development using a 1:5 solution of ethylcellusolve acetate and isopropyl alcohol.[9] The exposures are obtained in the direct beam without any filter. The lower exposure scale is obtained by assuming again an exposure rate of $35W/cm^3$.

V. Critical Parameters

a) Wafer Heating

The higher flux from a synchrotron or storage ring heats the mask/

wafer combination more than a conventional x-ray source. Different expansions of the masks and wafers during the exposure could cause a loss of resolution and make high-power, dedicated storage rings useless for lithography. For this reason, we have measured the temperature rise of silicon wafers exposed to the full beam of synchrotron radiation in vacuum and in about one torr of helium. A 1500 Å thick Al window is used for exposures in helium. This Al window is supported by a grid with a transmission of 80%. The one inch diameter silicon wafer is pressed against the standard mask mounting ring[5] by a teflon plug with no additional heat sink, or with a copper disk of 35g as a heat sink between the teflon plug and wafer. The mounting with the heat sink is the same as that used for copying a mask on a wafer. A thermocouple is cemented to the front of the wafer for the measurement of the temperature rise. The experimental results are summarized in Table III. Temperature rises of about 3°K are observed with the samples in vacuum; the heating is reduced by one order of magnitude with the samples in one torr of helium exchange gas. The time constant for the temperature rise in vacuum is longer than the exposure time necessary for PMMA. Therefore, no higher temperature rises during an exposure will occur if wafers are exposed to the more powerful radiation of a storage ring. The temperature will rise faster, but because shorter exposures are required the temperature at the end of an exposure is nearly independent of the intensity of the source, as long as the exposure time is long enough to equilibrate temperature differences between the mask and the wafer.

The calculated initial temperature rise for our standard mount (with copper heat sink) is 0.025°C/second and is in reasonable agreement with

the observations. The data given in Table III represents the worst case conditions: the wafer was exposed to the full beam of the synchrotron. Only a small spectral range (see Figs. 4 and 5), however, contributes to the exposure. Therefore, one can reduce the heating during exposure by prefiltering the radiation or, for example, by the use of a dedicated source where the radiation spectrum matches the effective resist absorption.

We have copied 1 μ linewidth masks with the full synchrotron beam and the standard mount in helium and in vacuum. In no case was any loss of resolution due to thermal expansion observed. We conclude that a heating of our mylar substrate will not limit the resolution of lithography even if much higher intensities and shorter exposure times are used. Our results do not allow general conclusions about the thermal expansion of other possible mask substrates.

b) Radiation Damage

Radiation damage to the substrate of an x-ray mask is expected to limit the useful life e.g. the number of replications obtained from one mask. No such damage had been observed with the AlKα radiation, but no mask had been exposed for more than the equivalent of 50 replications. The higher flux of a synchrotron permits the exposure of masks to much higher doses in a much shorter time. We have exposed one mask to the full beam of DESY for several increasing doses, with a total dose equivalent to 10^4 exposures. After each dose a copy of the mask was made on a silicon wafer. These copies were developed and the distance between identical lines were measured using a Moore measuring machine. No change in the distance with increasing dose could be detected. The mean error of the distances (about

0.25 μm over a 8 mm distance) was the same as that obtained for a mask which had been exposed only to a low total dose. However, after a total dose equivalent to $\sim 5 \times 10^6$ J/cm^3 (or 10^4 replications with PMMA resist), radiation damage to the mask could be clearly recognized by a yellow coloration of the mylar.

VI. Summary and Conclusions

We have used synchrotron radiation from DESY in Hamburg for the replication of x-ray masks on silicon wafers. DESY is not optimized for x-ray lithography in that its spectrum contains very hard radiation for which thin high resolution masks have low contrast. For this reason, replicas have been produced not only with the full beam but also with modified beams which did not contain hard x-ray radiation. DESY operated during our visit at a low current of 8 ma (1/10 of the maximum); exposure times ranged from about 30 seconds to 3 minutes for the replication with vertical walls of masks on 6 μ thick mylar substrates.

Our experimental results can be summarized as follows:

1) High resolution replication of masks down to linewidths of 500 Å can easily be obtained with synchrotron radiation.
2) Masks with thin absorber films ($t < 1000$ Å) which can be easily produced with high resolution using e-beam techniques can be copied if sufficiently soft radiation is used.
3) The distance between mask and wafer is not critical; distances up to 1 mm have been used for the replication of a 1 μ linewidth magnetic bubble patterns.

4) PMMA and a more sensitive experimental resist have been evaluated with synchrotron radiation. Cross linking of PMMA has been observed for exposures of 10^5 J/cm^3.

5) Heating of the mask and wafer by the radiation did not have any deleterious effect on resolution. The thermal time constant for heating can be made larger than the required exposure time. Therefore high intensity dedicated storage rings which allow much shorter exposure times need not produce larger temperature rises during the exposure.

6) A mylar mask exposed to the full beam for an equivalent of 10^4 replications showed radiation damage as a yellow color. No change in dimensions of the mask due to this radiation damage could be detected.

We conclude that storage rings are very desirable light sources for x-ray lithography. For multilevel structures with alignment, a storage ring is far superior to a conventional source due to its collimation and intensity which make the distance between mask and wafer uncritical and allow for short exposure times.

Appendix A. General Considerations of Storage Ring Sources for X-ray Lithography

In this Appendix, we describe various factors (mask considerations, absorption properties of resists, etc.) relevant in optimizing storage ring radiation sources for x-ray lithography and suggest what an optimized source might look like. A comparison with conventional x-ray tube sources is also given, illustrating the unique power and brightness characteristics of synchrotron radiation sources.

Before discussing these subjects, we give the formula for the spectral distribution of synchrotron radiation, which forms the basis for the spectral calculations described here. For a storage ring in which the electron energy is E and the magnetic radius R_M, the total output power of the entire storage ring in watts/eV of photon energy for a 1 ampere circulating beam is[11]

$$\frac{dP}{d(h\nu)} = 1.23\times10^{8} \frac{E^{7}}{(h\nu)^{2}R_M^{2}} G\left(\frac{h\nu}{h\nu_c}\right) \tag{1}$$

where E is in GeV, the photon energy $h\nu$ is in eV, and R_M, which is in meters, is given in terms of the magnetic field strength H by

$$R_M = 33.4 \frac{E[\text{GeV}]}{H[\text{kOe}]} . \tag{2}$$

The "critical photon energy" $h\nu_c = \frac{hc}{\lambda_c}$ corresponds to wavelength λ_c, where the critical wavelength λ_c is given by

$$\lambda_c[\mathring{A}] = \frac{187}{H[\text{kOe}]E^{2}[\text{GeV}]} \tag{3}$$

The critical wavelength determines the wavelength range where the spectral output is greatest, as can be seen from Fig. 3, or from Eq. (1) and Fig. 14. For $\lambda << \lambda_c$, (or $h\nu >> h\nu_c$) the radiated power/eV decreases extremely rapidly with increasing $h\nu$(e.g. $dP/d(h\nu)$ - Eq. (1) - varies as $(h\nu)^{-1/2} e^{-h\nu/h\nu_c}$ in this range). Finally, the "universal function" G(y) appearing in (1) is defined by

$$G(y) \equiv y^3 \int_y^\infty dx K_{5/3}(x) \tag{4}$$

where K_ν is the modified Bessel function of the second type. Formulae 1-3, together with a plot of G(y) (Fig. 14), provide a useful description of the spectral source characteristics of synchrotron radiation. The radiation power given by Eq. (1) is distributed over 2π radians in the horizontal plane (being emitted only from regions (bending magnets) where the electron trajectories curve, and is collimated vertically so as to be confined to a vertical angle (in milliradians) of about E^{-1}, where E is in GeV.

At present, there are about eleven synchrotrons and four storage rings in operation which have an electron energy range useful for x-ray lithography ($E \gtrsim 0.6$ GeV). (See e.g. Table I in Ref. 10, p. 253). These include the powerful 4.0 GeV storage ring at the Stanford Linear Accelerator Laboratory, the 12 GeV synchrotron at Cornell, as well as the 7.5 GeV DESY synchrotron and the more powerful 3.5 GeV DORIS storage ring at DESY, Hamburg, Germany. To date, all of these storage rings and synchrotrons of energy $E \gtrsim 0.6$ GeV have been built for high energy physics. Synchrotron radiation is obtained in a parasitic way at one or more ports on these big machines. The construction of electron storage rings designed solely as

radiation sources, e.g., the 2 GeV ring planned at Daresbury, has gained support in recent years. Such sources can be both smaller and less expensive than most existing synchrotron radiation sources while at the same time delivering a higher usable flux. In addition, the emitted spectrum of a dedicated source can be matched to the needs of the user. As one of many benefits, such designs can eliminate undesirable radiation hazards due to hard x-rays.

We now consider spectral requirements of the lithography process and show how well these requirements can be met with optimized storage ring sources.

Three parameters govern the lithography efficiency and quality for photons of energy $h\nu$. If T_A is the transmission of the mask absorber, T_S that of the mask substrate, and A_R is the absorption of the x-ray resist, then $T_S A_R$ is the fraction of incident photons absorbed by the x-ray resist, in regions where exposure is desired. Similarly, $T_A T_S A_R$ is the fraction of photons absorbed by the x-ray resist in regions which are to be masked. In an optimum design for lithography, the range of $h\nu$ and the materials chosen are such that $T_S A_R$ and the contrast $(1/T_A)$ are maximized, while $A_R \simeq 0.63$. The last condition insures that the absorption of photons at the bottom of the resist is maximized. Fig. 12 shows A_R as a function of photon energy $h\nu$ for two x-ray resist thicknesses. We will see below that most of the radiation is emitted at energies $h\nu \lesssim 1000$ eV for storage ring parameters considered here. Under these conditions, mask absorber materials (such as Au), have optical absorption depths of $\lesssim 0.1\ \mu$, and T_A can be made small, $T_A \gtrsim 0$. A particular advantage of working in the very soft x-ray range (say

$250 \lesssim h\nu \lesssim 1000$ eV) is that high contrast masks ($T_A << 1$) can be readily made using e-beam techniques with thin layers of absorbers such as Au.

In a storage ring optimized for x-ray lithography, the electron energy E, magnetic field H, and beam current I are chosen to minimize cost while still providing reasonable flux in the relevant wavelength region. Previous studies have determined that magnetic fields of $\sim$ 1.2 tesla (12 kOe) are most cost-effective for machines of the size we will consider. Assuming this value for the magnetic field H, one can plot the spectral distribution of power delivered to a lithography exposure station, for various choices of E. This spectral output is shown in Figs. 3 and 13 for values of E of 0.7 and 1.0 GeV. Also shown in Fig. 13 are two photoresist + mask response curves ($T_S A_R$ vs. $h\nu$).

We now discuss the advantages of storage ring sources for lithography requiring precision registry between two or more exposures. One of the important limiting factors of the registration process is the difficulty in controlling the value of mask-photoresist distance a (Fig. 1), due to a variety of factors. In general, the registration problem becomes easier as the collimation of the source increases. If R is the source distance then an error δa in mask-photoresist distance leads to an error δD in the transverse spacing of two exposed elements on the wafer given by: $\delta D = \frac{D}{R} \delta a$. For example, if we require that $\delta D \leq 0.1\mu$, $D = 5$ cm, and $R = 5$ meters for a storage ring and 30 cm for an x-ray tube, then $\delta a \lesssim 10\mu$ for a storage ring but $\delta a \lesssim 0.6\mu$ for an x-ray tube source - a tolerance 15 times more stringent.

There are other geometrical requirements in x-ray lithography which are less severe with the large distance between source and wafer (R in Fig. 1) available using a storage ring. For example, finite source size (of diameter d in Fig. 1), leads to a penumbra of total width $\delta w = ad/R$ (δw = image spread due to finite source size). For a required value of δw, the storage ring case (exposing at 5 m) leads to a maximum mask-wafer spacing which can be $\sim$ 15 times as great as for the x-ray source at 30 cm, or equivalently a less stringent requirement on source size. This has been demonstrated in Section IV. The main point is that since x-ray lithography is a lensless, shadow casting method, many geometrical restrictions are amenable to solution by increasing the exposure distance. This is an available route for the high-intensity storage ring, but can quickly lead to impossibly long exposure times for the conventional x-ray source.

We note that while some aspects of the multiple-exposure transverse registry problem are not yet solved, the source characteristics of an electron storage ring simplify the problems and can be used in developing a viable solution. As previously mentioned, significant advantages of synchrotron radiation sources are the reduction of exposure time and increased flexibility of exposure geometry with a storage ring.

The synchrotron radiation is spread vertically by $\delta\theta_v \sim 1.7 \times 10^{-3}$ radians for a 0.6 GeV storage ring (the lowest energy ring likely to be considered as a dedicated lithography source), so that wafers can be exposed by moving them vertically through this flat beam of radiation. If we assume as a typical case an exposure station 5 meters from the ring and a beam line 3.6° wide horizontally, then $\sim$ 3.4 watts is radiated into a processing area

of size 30 cm wide by $\sim$ 1 cm high in the $200 \leq h\nu \leq 2000$ eV range, the energy range where the machine spectrum and photoresist-mask response are greatest (see Fig. 13).

Figure 12 also shows that $\sim$ 0.1 of these photons (i.e. $\sim$ 0.34J/sec.) are absorbed in the photoresist, so this one processing area can produce about 1×10^{-2}J/sec-cm^2 of actual energy used in exposing photoresist, available over the 30 cm^2 area.

By comparison, a 4 kW Al-Kα x-ray tube produces $\sim$ .4Jj/sec of photons at 1487 eV, of which only a fraction $\lesssim \frac{1}{4}$ are usable (those in a cone of $\sim$ 60° total width, due to electrode shadowing. A typical exposure distance is $\lesssim$ 30 cm (to keep exposure times short - of the order of several hrs. to 1 day), and about .05 of the incident photons are absorbed by the photoresist in this model (see Fig. 13), giving finally 5×10^{-6}J/sec-cm^2 over an area of $\sim$ 900 cm^2, or 0.005 J/sec total energy used in exposing resist.

These comparisons, for one typical set of various parameters, show that output in the relevant photon energy range from 1% of the storage ring is $\sim$ 30 times that of one high-power x-ray tube ($\sim$ 2000 times as bright), can be concentrated by a factor of $\gtrsim$ 30 in area, and is twice as efficient for this mask-photoresist combination, giving an exposure rate increase per chip of $\sim$ 2000 for any given exposure. For example, a typical exposure taking 6.5 hr. with an x-ray tube source will take $\sim$ 15 seconds with the storage ring. As shown in Fig. 4 of Ref. 5, this exposure corresponds to a very heavy exposure, giving a development rate ratio of better than 125:1 between exposed and unexposed resist using PMMA (2041) and resulting in

sharp vertical wall patterns. By using such heavy exposures, development requirements become minimal.

References

1. B. L. Henke and E. S. Ebisu, "Low energy x-ray and electron Absorption within solids", AFOSR Report 72-2174, Univ. of Hawaii, Aug. 1973.

2. B. L. Bracewell and W. J. Veigele in Developments in Applied Spectroscopy, Vol. 9, edited by E. L. Grove and A. J. Perkins, (Plenum, New York, 1971), p. 375.

3. H. J. Hagemann, W. Gudat, and C. Kunz, J. Opt. Soc. Am. 65, 742 (1975).

4. H. I. Smith, D. L. Spears, and S. E. Bernacki, J. Vac. Sci. Tech. 10, 913 (1973).

5. E. Spiller, R. Feder, M. Heritage, L. Romankiw, J. Topalian, and E. Castellani, "Fabrication of Bubble Devices with X-ray Lithography", Solid State Technol., April 1976, p. 62.

6. E. M. Rowe et al. Proc. Nat. Accel. Conf. (Chicago, March 1-3, 1971), pages 210-212; E. M. Rowe and F. E. Mills, "Tantalus I: A Dedicated Storage Ring Synchrotron Radiation Source", Particle Accelerators 4, 211 (1973).

7. M. Hatzakis, J. Electrochem. Soc. 116, 1033 (1969).

8. R. Feder, I. Haller, M. Hatzakis, L. T. Romankiw, E. Spiller, (private communication) and I. Haller, R. Feder and E. Spiller (to be published).

9. Experimental resist 76/24, batch 859704-49 provided by E. Gipstein, IBM Research, San Jose.

10. E. Koch, R. Haensel and C. Kunz, Editors, Vacuum Ultraviolet Radiation Physics, (Pergamon, Vieweg, Braunschweig, 1974).

11. E. M. Rowe, "Tantalus II" in Research Applications of Synchrotron Radiation, R. E. Watson and M. L. Perlman, editors, Brookhaven National Laboratory Report BNL-50381, (Brookhaven National Laboratory, N.Y., 1973), C. Gahwiller, F. C. Brown, and H. Fujita, Rev. Sci. Instr. 41, 1275 (1970).

Figure Captions

Fig. 1: Illustration of the basic components of the x-ray lithography process.

Fig. 2: Schematic diagram of the experimental arrangement at DESY.

Fig. 3: Radiation flux from three synchrotron radiation sources. Curve a.) is the flux from DESY 40 m from the source at 3.5 GeV maximum electron energy and with an 8 ma beam current, which approximates the conditions used for the experiments described in this paper. In practice, at least three factors can modify this curve at DESY. One is the time structure of the electron energy, as DESY is a synchrotron and not a storage ring. Secondly, the mirror described in the text modifies this distribution. Finally, maximum beam currents of close to a factor of 10 higher than the 8 ma assumed here have been used at DESY at different times. Curves b.) and c.) represent the unfiltered radiation flux from 1.0 and 0.7 GeV electron storage rings, 10 and 7 meters from the source, with 12 kOe magnetic fields and 100 ma beams.

Fig. 4: Power absorbed in resist (PMMA) as a function of wavelength for synchrotron radiation from DESY (3.5 GeV, 8 ma) 40 m from electron orbit for various filters in the beam. (a) no filter; (b) 0.3 μ of PMMA; (c) 1.5 μ of Parylene N; (d) 1 μ of PMMA; (e) 12 μ of beryllium; (f) 6 μ of mylar; (g) 6 μ of mylar + 0.8 μ of gold.

Fig. 5: Calculated power absorbed in resist (PMMA) for synchrotron radiation from DESY (3.5 GeV, 8 ma) after reflection from gold at a glancing angle of 4°. (a) no filter, (b) filter of 1 μ thick PMMA, (c) 1.5 μ of parylene N (d) 2.5 μ of mylar.

Fig. 6: Mask replication (1 μ linewidth) with various distances between mask and wafer: Filter: 12 μ Be + 6 μ mylar, exposure time: 3 min, effective exposure 250/j/cm^3, resist: PMMA 2041 mask-wafer spacing d and gold thickness t in mask. (a) d = 0.14 mm, t = 0.7 μ; (b) d = 0.54 mm, t = 0.5 μ; (c) d = 1.04 mm, t = 0.7 μ.

Fig. 7: Replication of 1 μ linewidth mask with low effective contrast:

(a) Filter: 6 μ mylar, exposure time 30 sec ≡ 78 J/cm^2 resist 76/24 copolymer, t_{Au} = 0.8 μ; effective contrast of mask 6:1

(b) Filter 6 μ mylar, exposure time 3 min ≡ 450 J/cm^3; resist: PMMA, t_{Au} = 0.35 μ, effective contrast of mask: 3:1

(c) Filter: 75 μm Si: exposure time 170 min ≡ 80 J/cm^3 resist: 76/24 copolymer, t_{Au} = 1.4 μ, effective contrast: 2.3:1. In this exposure the pattern was transferred from the back to front of a 75 μm thick silicon wafer.

Fig. 8: Power absorbed in resist (PMMA) as a function of wavelength for synchrotron radiation from DESY (3.5 GeV, 8 ma) filtered by 75 μ of silicon (a) and by 75 μ of silicon and 1.4 μ of gold (b).

Fig. 9: Replication of high resolution patterns with soft radiation:

(a) & (b) Fresnel zone plate with 700 Å smallest linewidth and t_{Au} = 0.1 μ in the mask; filter: 4° glancing angle gold mirror + 1.5 μ parylene N, exposure time: 25 min, effective exposure: 3000 J/cm^2 calculated with optical constants of gold from Ref. 7, resist PMMA.

(c) Detail of diatom: filter 4° gold mirror, exposure time 10 min, effective exposure about 1200 J/cm^3; exposure non-uniform through resist thickness, resist PMMA.

Fig. 10: Dissolution rate versus exposure for heavily exposed PMMA. Developer is MIBK diluted with isopropyl alcohol; points with an arrow represent a lower limit to the dissolution rate: for these points the exposed resist was completely removed in the time required to immerse, remove and dry a wafer and a more dilute developer was required. At exposures above 10^5 J/cm^3 the exposed parts of the resist are less soluble than the unexposed parts; concentrated MIBK is used as a developer and the resist becomes negative.

Fig. 11: Dissolution rate versus exposure of 76/24 copolymer, baked one hour at 230°C. and developed in a 1:5 solution of Ethyl cellusolve acetate and isopropyl alcohol. Top scale exposure time in the direct unfiltered beam in vacuum. Bottom scale obtained with the assumption of 35 W/cm^3.

xxx: D. R. obtained from initial slope

●●●: D. R. obtained from average slope

+++: D. R. obtained from final slope

□ : Sample exposed through a filter of 12 μ Be

Fig. 12: The fraction A_R of photons incident on a.) 0.5 μ thick and b.) 1.0 μ thick x-ray resist which are absorbed in the resist as a function of photon energy.

Fig. 13: The factor $A_R T_S$, which represents the fraction of the radiation incident on the "clear" areas of a mask which are absorbed in 1 μ thick resist are plotted in curves a.) and b.) as a function of photon energy. Curve a.) is for a 2 μ thick mylar mask substrate, while curve b.) is for a 6 μ mylar mask. Curves c.) and d.) correspond to curves c.) and a.) of Fig. 3, and represent the intensity of radiation emitted by synchrotron radiation sources which possess rather "soft" (curve c.) and "hard" (curve d.) output spectral distributions.
Note that curves a.) and b.) represent the response only of the mask + resist, while Figs. 4 and 5 combine this response with the filtering action of the 4° Au mirror at DESY. Thus Figs. 4 and 5 represent the actual situation for the experiments reported in this paper, while the present figure represents the "ideal" response of the basic components of the lithography process itself.

Fig. 14: The function G(y) vs y, used in determining the spectral distribution of synchrotron radiation. (See appendix).

FILTER	EFFECTIVE EXPOSURE RATE ($J/cm^3 sec$)
Direct beam, no filter	74 ($0 < \lambda < 120$ Å)
direct beam 0.3μ PMMA	36 ($0 < \lambda < 120$ Å)
" 1μ PMMA	13
" 1.5μ Parylene N	11.5
" 12μ Beryllium	2.8
" 6μ Mylar	2.6
" 6μ Mylar + 0.8μ gold	0.44
" 75μ Silicon	8.4×10^{-3}
" 75μ Silicon + 1.4μ gold	3.6×10^{-3}
4° beam, no filter	30 ($0 < \lambda < 120$ Å)
" 1.5μ Parylene N	2
" 2.5μ Mylar	0.9
" 1.5μ Parylene N + 0.1μ gold	

Table I - Effective exposures of resist (PMMA) by synchrotron radiation from DESY (3.5 GeV, 8 ma) for various filters. In unfiltered radiation, a large contribution to the exposure comes from very soft x-rays which expose only a very thin layer at the top of the resist. The contribution of wavelengths above 120 A has therefore not been included in the table.

MASKS	1μ linewidth bubble pattern, t_{Au} = 0.35-3μ. Fresnal zone plate, 0.07μ smallest linewidth, t_{Au} = 0.1μ Diatoms, finest structures ∿0.05μ
Mask - Wafer Distance	0 - 0.075 - 0.14 - 0.28 - 0.52 - 1.04 mm
Resist	2041 PMMA, 76/24 experimental resist
Spectral Filters	no filter, 6μ mylar, 6μ mylar + 12μ Be, 6μ mylar + 0.15μ Aℓ, 4° glancing angle gold mirror, 4° mirror + 1.5μ Parylene N, 75μ silicon
Exposure times	2 sec - 4 hrs.
Effective Exposures	5 - 100,000 J/cm^3 exposures in Vacuum or 1 Torr of He.

Table II - Ranges of parameters used in the replication of masks with synchrotron radiation

EXPOSURE CONDITIONS	TEMPERATURE RISE	TIME CONSTANT
a) Vacuum, 1" silicon wafer (no heat sink)	3.3°C	3 min
b) Vacuum, standard mount silicon, 35g Cu heat sink	3.5°C	5 min
c) 1 Torr He, Aℓ-window, 0.15μ thick, no heat sink	0.5°C	30 sec
d) 1 Torr He, Aℓ-window 0.15μ thick, standard mount, 35g Cu heat sink	0.2°C	10 sec

Table III - Measured temperature rises of 1" diameter silicon wafers exposed for a long time to the full beam from DESY operating at 3.5 GeV and 8 ma. Calculated flux from DESY is ~ 0.195 W/cm^2 averaged over an area of 10x20 mm^2.

THE X-RAY LITHOGRAPHY PROCESS

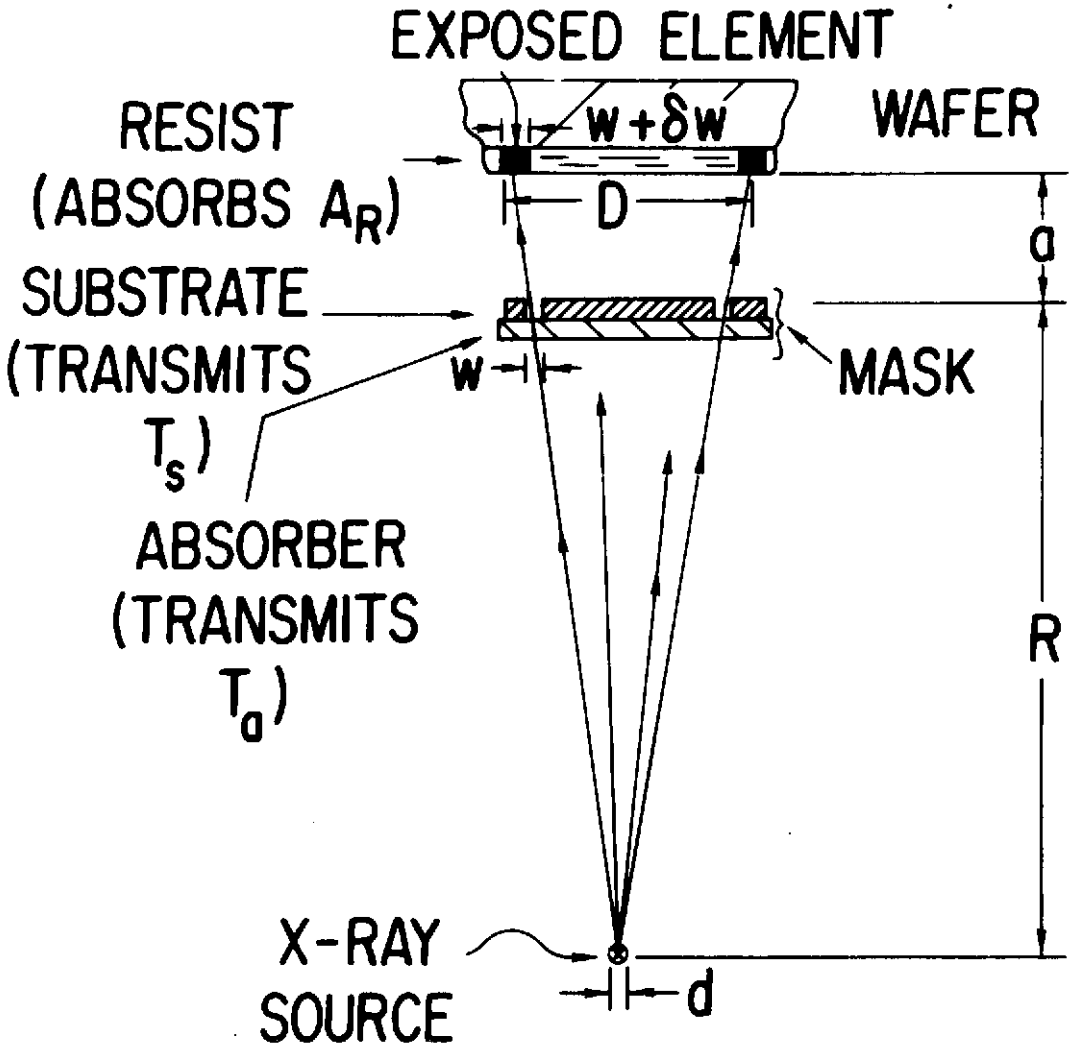

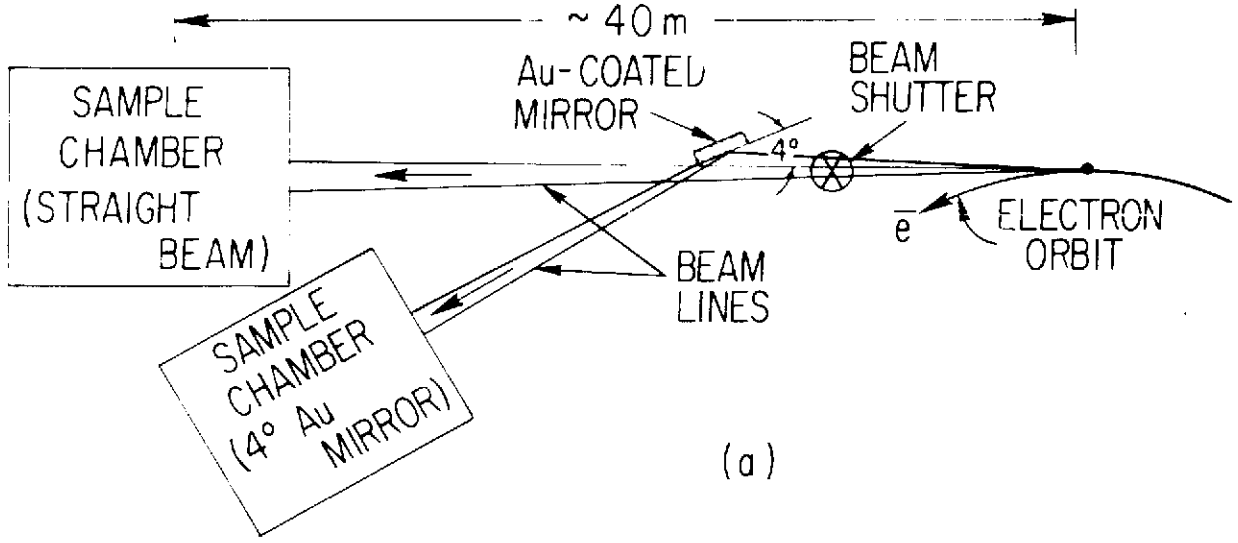
~ 40 m
SAMPLE CHAMBER (STRAIGHT BEAM)
Au-COATED MIRROR
BEAM SHUTTER
4°
e⁻
ELECTRON ORBIT
BEAM LINES
SAMPLE CHAMBER (4° Au MIRROR)

(a)

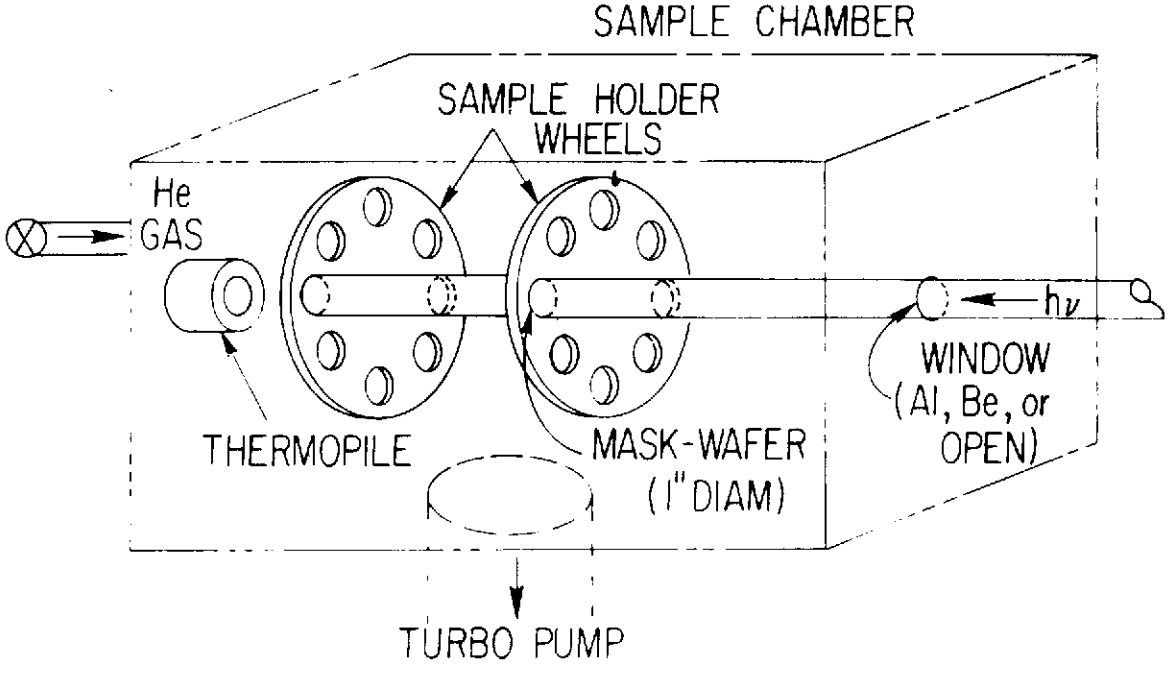
SAMPLE CHAMBER
SAMPLE HOLDER WHEELS
He GAS
hν
WINDOW (Al, Be, or OPEN)
THERMOPILE
MASK-WAFER (1" DIAM)
TURBO PUMP

(b)

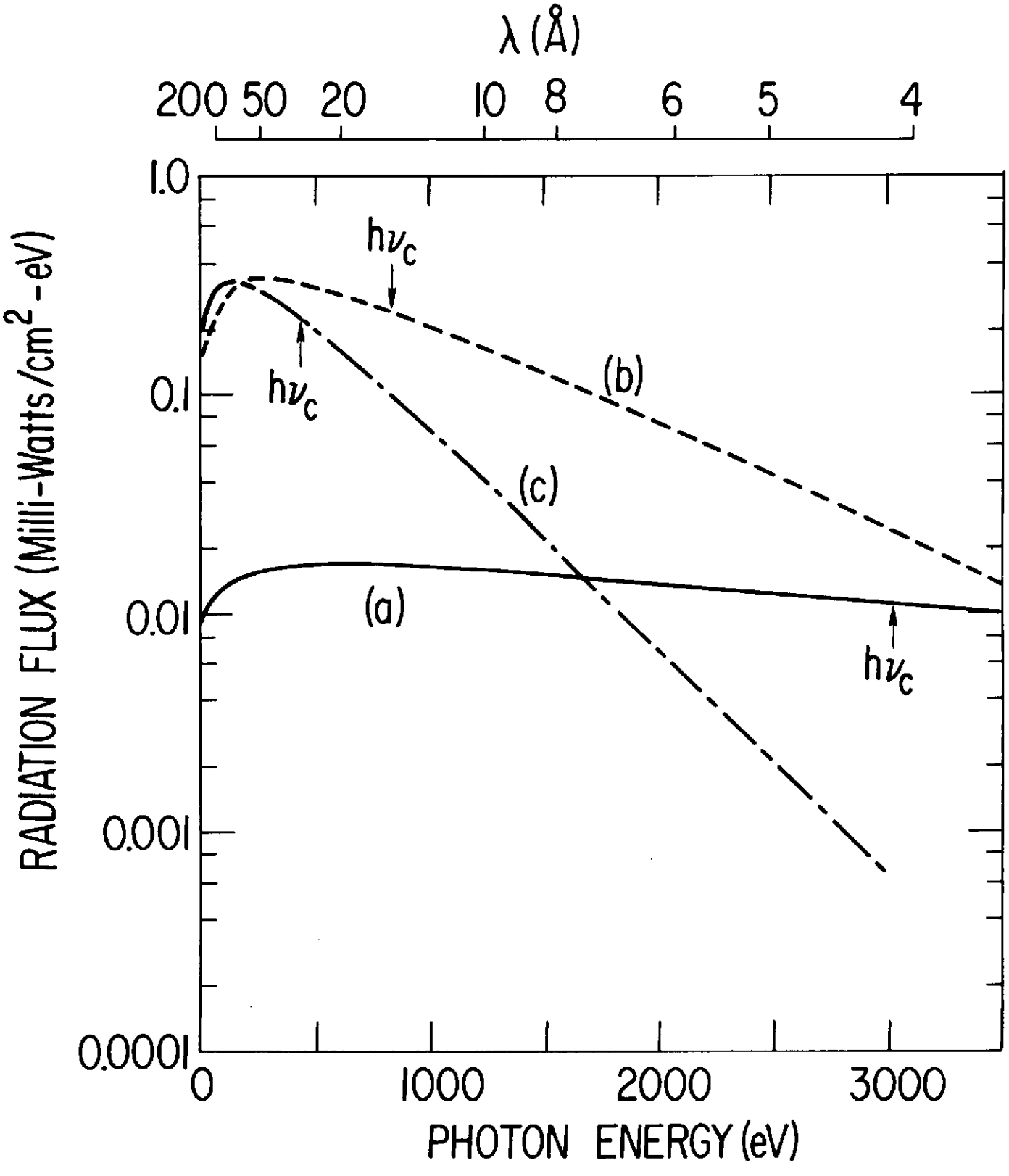
λ (Å)
200 50 20 10 8 6 5 4
1.0
0.1
0.01
0.001
0.0001
RADIATION FLUX (Milli-Watts/cm²-eV)
hνc
hνc
hνc
(a)
(b)
(c)
0
1000
2000
3000
PHOTON ENERGY (eV)

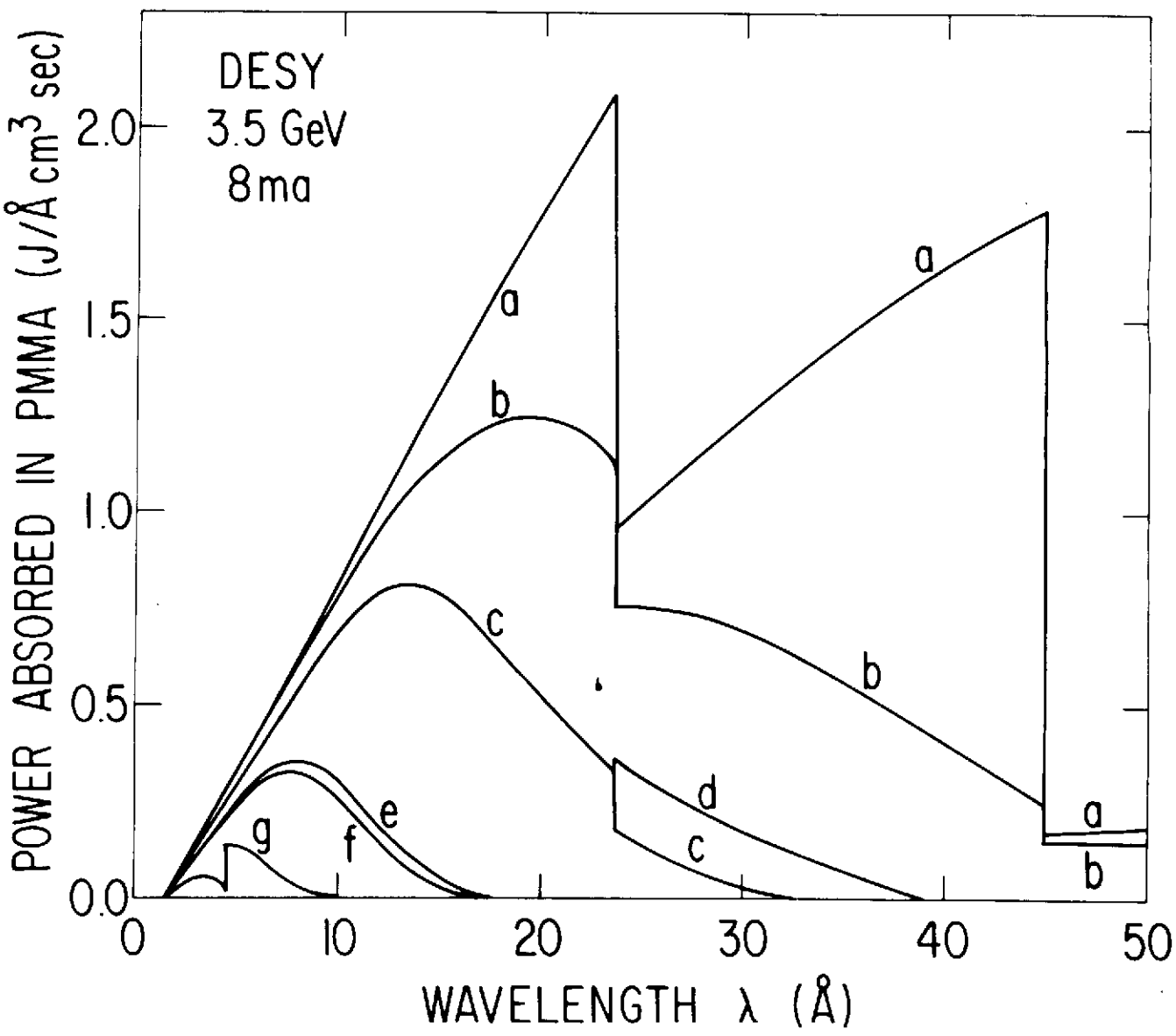
DESY
3.5 GeV
8ma
POWER ABSORBED IN PMMA (J/Å cm³ sec)
WAVELENGTH λ (Å)
0.0
0.5
1.0
1.5
2.0
0
10
20
30
40
50
a
b
c
d
e
f
g

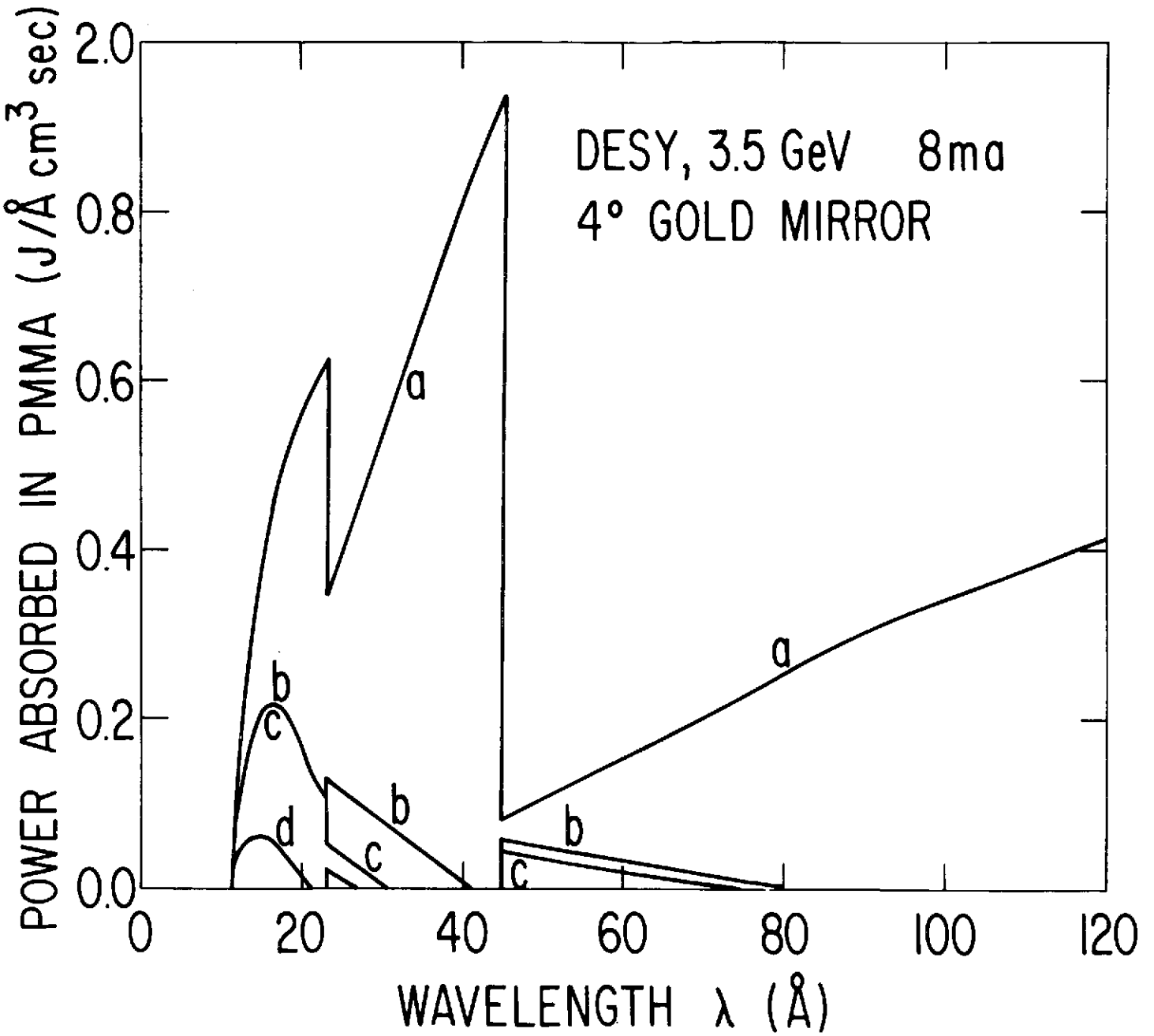
DESY, 3.5 GeV 8ma
4° GOLD MIRROR
POWER ABSORBED IN PMMA (J/Å cm³ sec)
WAVELENGTH λ (Å)
2.0
0.8
0.6
0.4
0.2
0.0
0
20
40
60
80
100
120
a
b
c
d
a
b
c
b
c
d
b
c

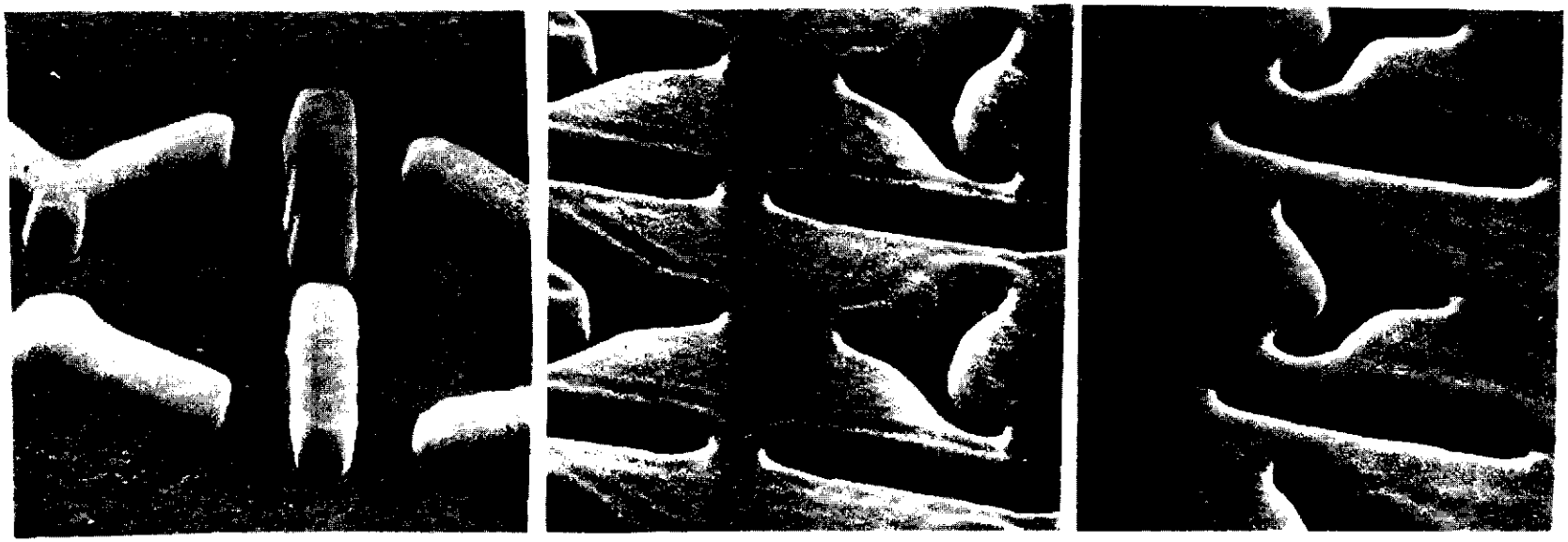

a b c

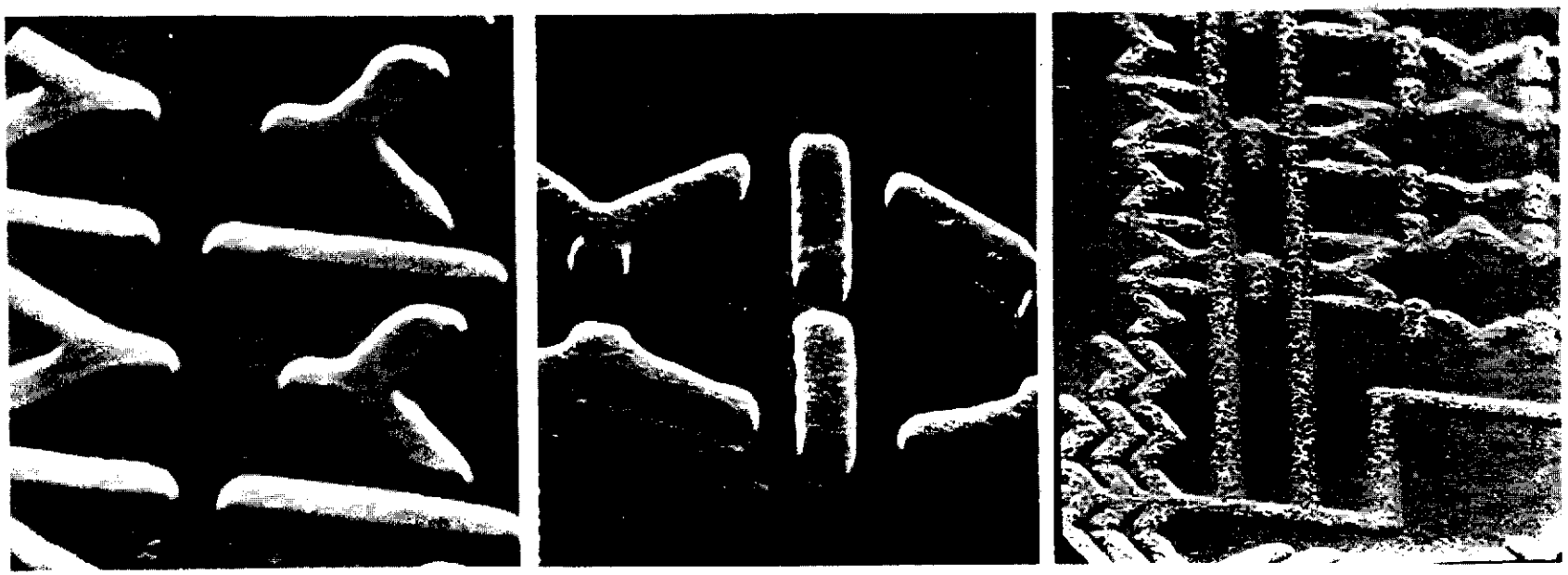

a b c

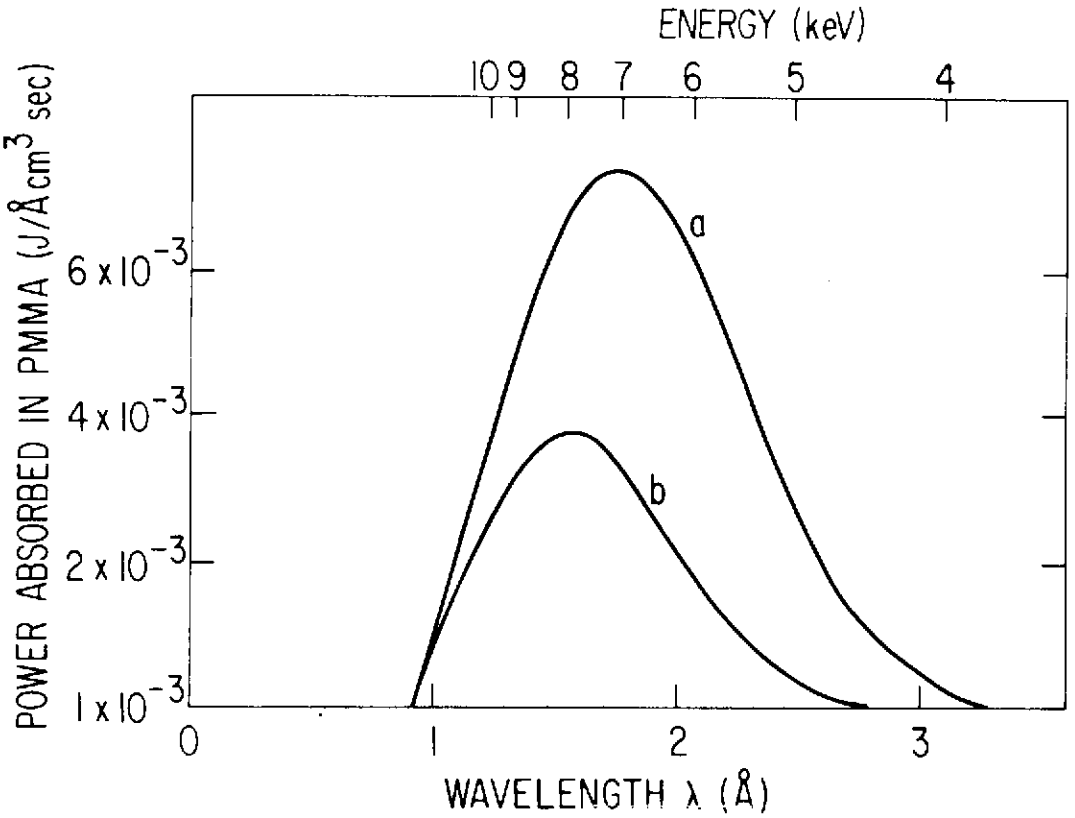
ENERGY (keV)
10 9 8 7 6 5 4
POWER ABSORBED IN PMMA (J/Å cm³ sec)
6 x 10⁻³
4 x 10⁻³
2 x 10⁻³
1 x 10⁻³
a
b
0
1
2
3
WAVELENGTH λ (Å)

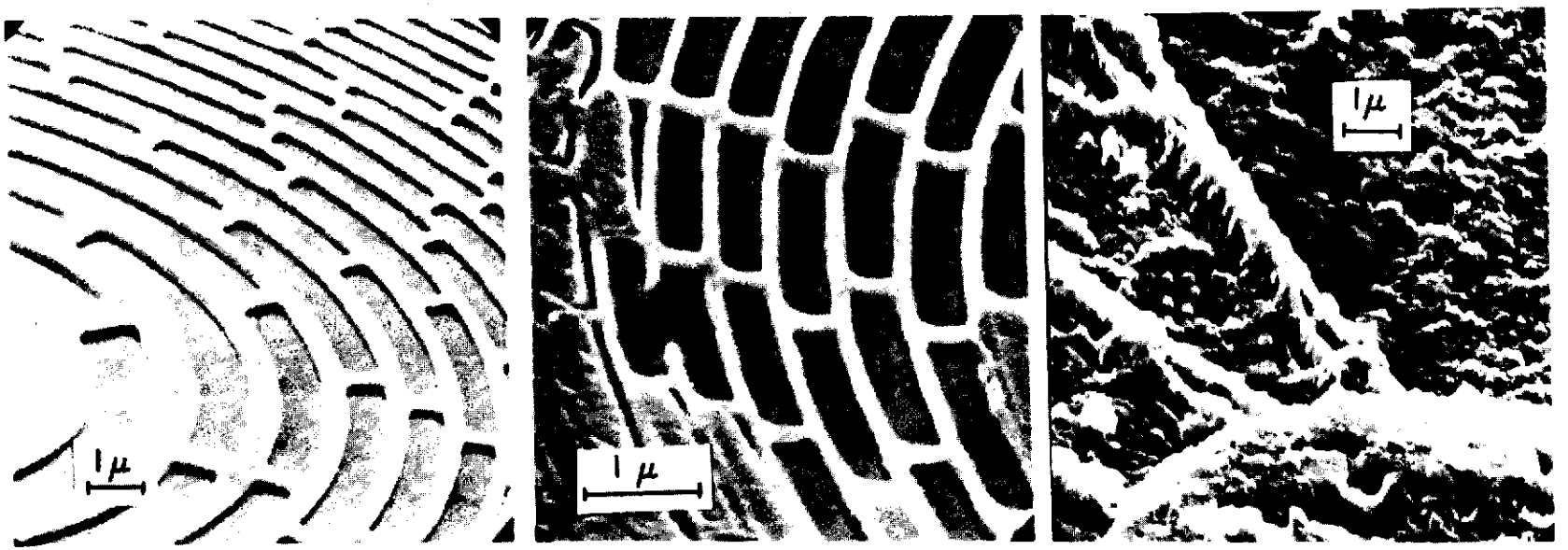

a b c

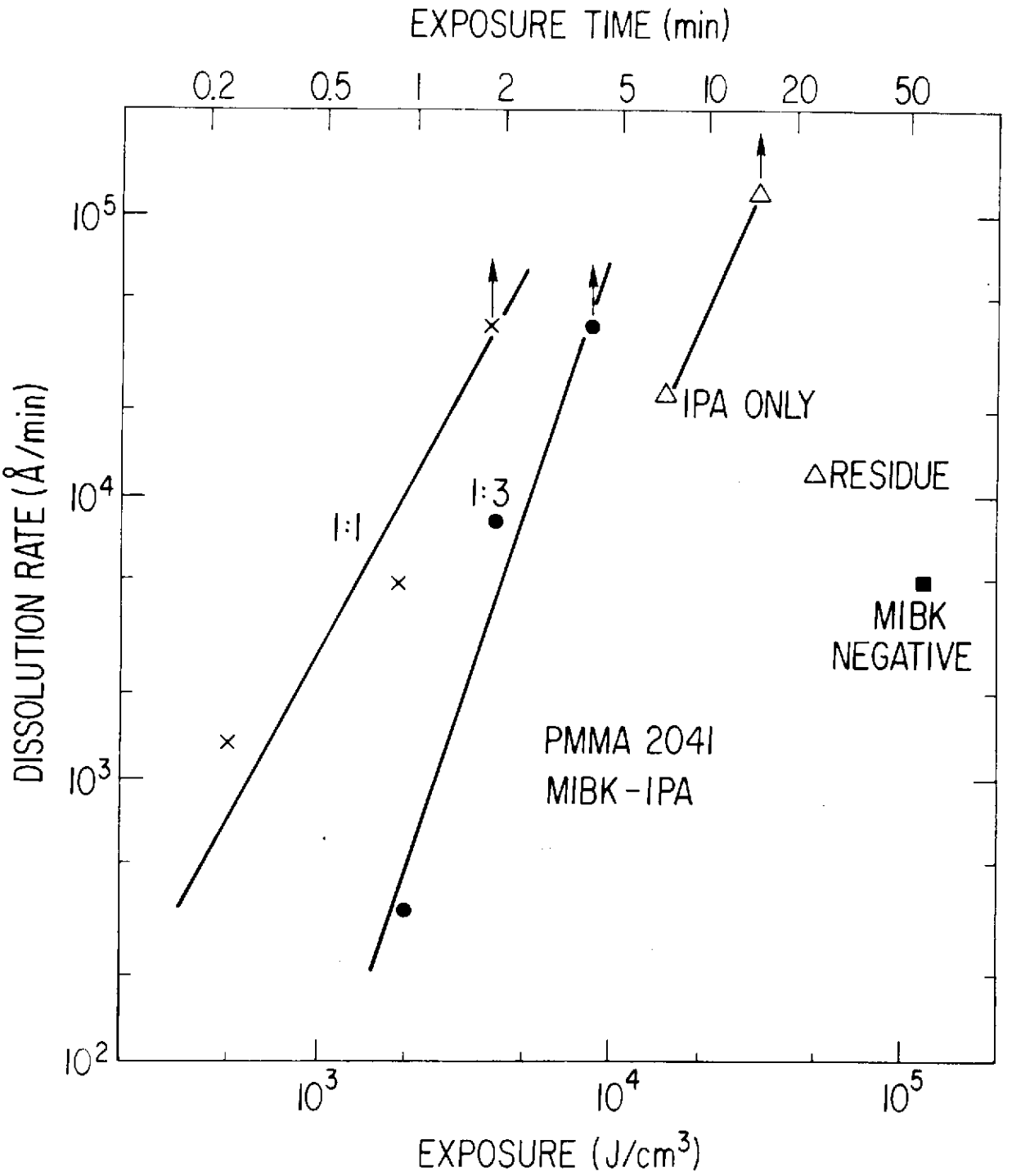
EXPOSURE TIME (min)
0.2
0.5
1
2
5
10
20
50
10^5
10^4
10^3
10^2
DISSOLUTION RATE (Å/min)
1:1
1:3
IPA ONLY
RESIDUE
MIBK
NEGATIVE
PMMA 2041
MIBK - IPA
10^3
10^4
10^5
EXPOSURE (J/cm^3)

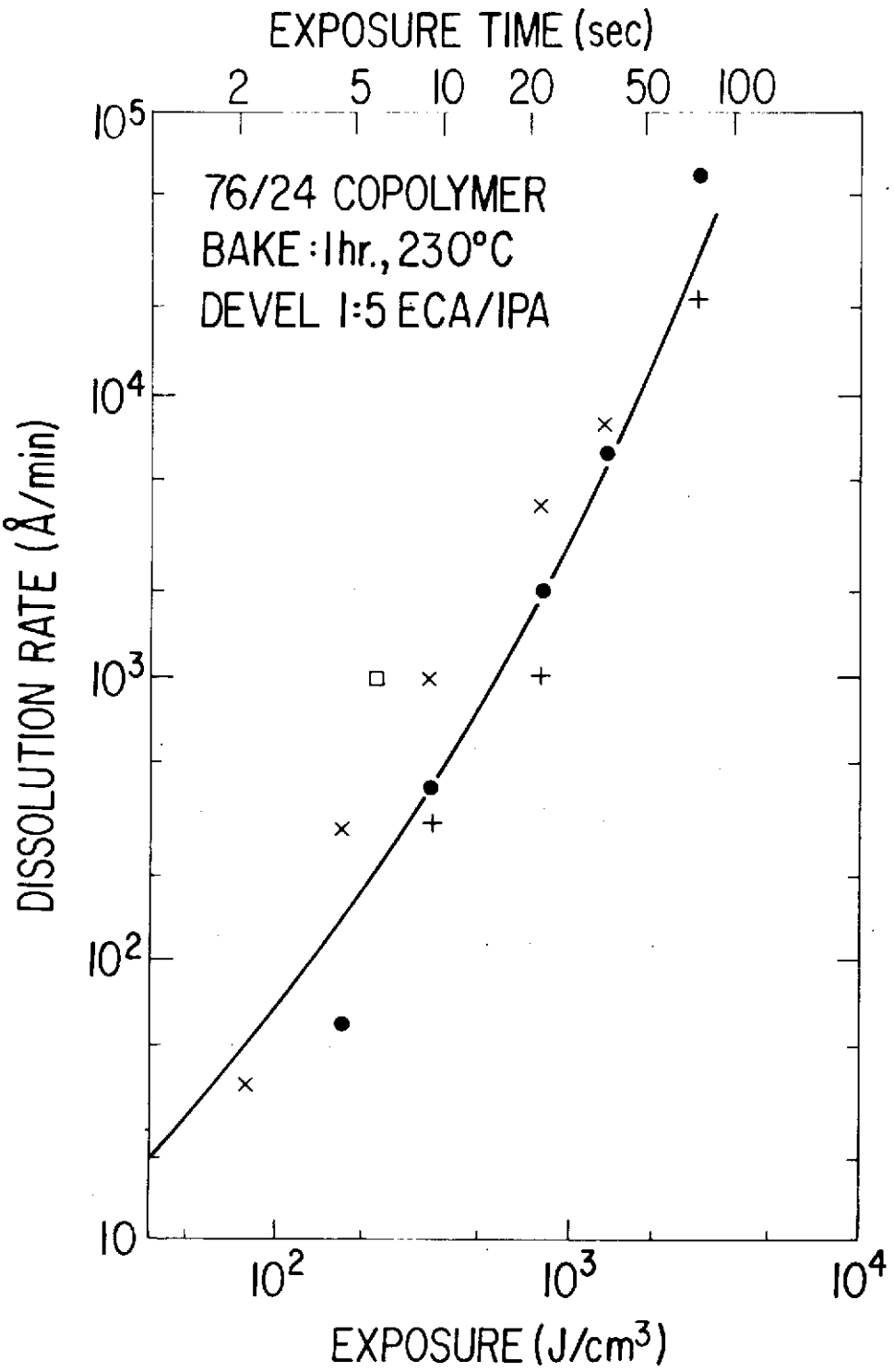
EXPOSURE TIME (sec)
2
5
10
20
50
100
76/24 COPOLYMER
BAKE: 1hr., 230°C
DEVEL 1:5 ECA/IPA
DISSOLUTION RATE (Å/min)
10^5
10^4
10^3
10^2
10
10^2
10^3
10^4
EXPOSURE (J/cm^3)

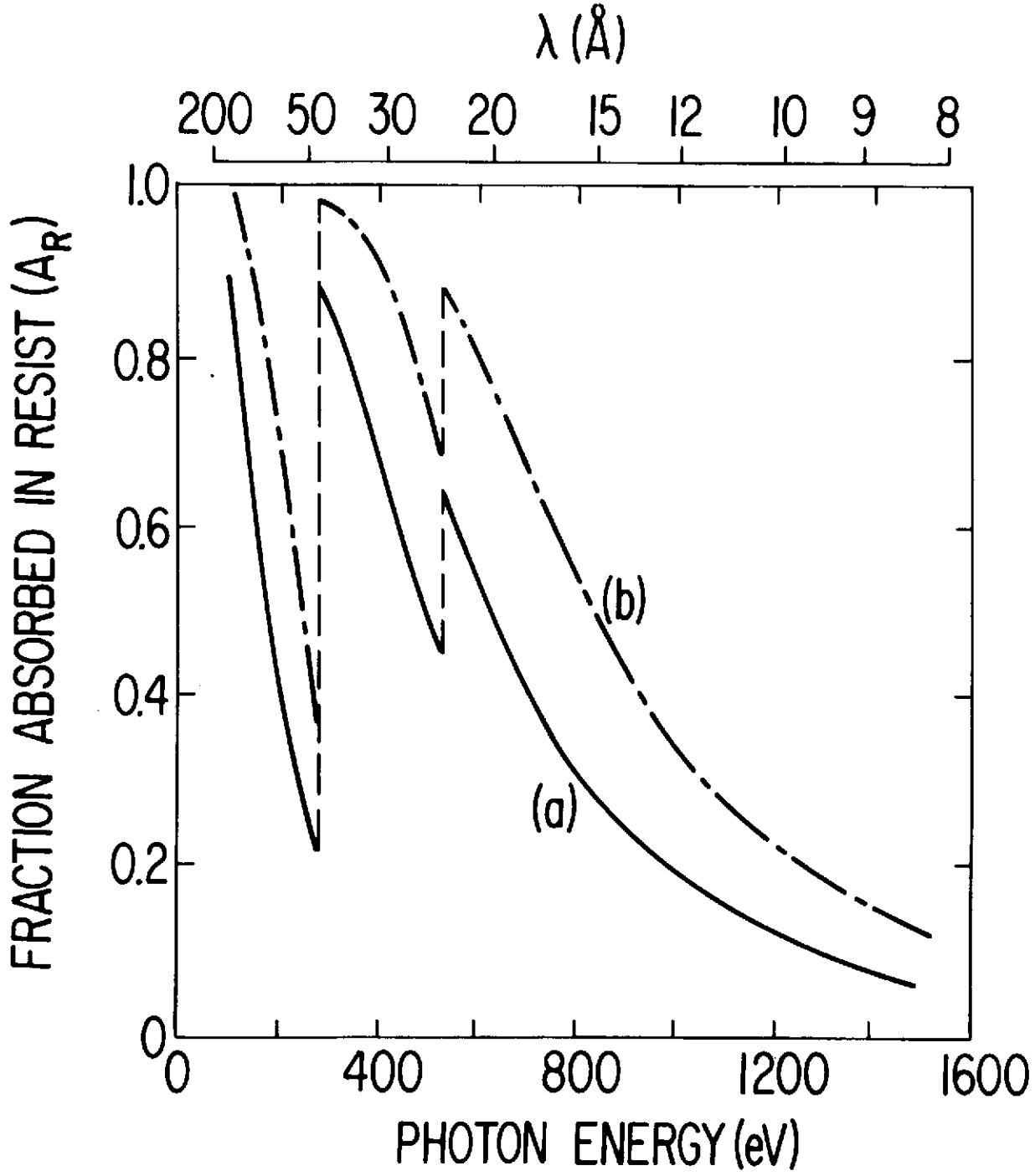
λ (Å)
200 50 30 20 15 12 10 9 8
1.0
0.8
0.6
0.4
0.2
0
FRACTION ABSORBED IN RESIST (A_R)
(a)
(b)
0 400 800 1200 1600
PHOTON ENERGY (eV)

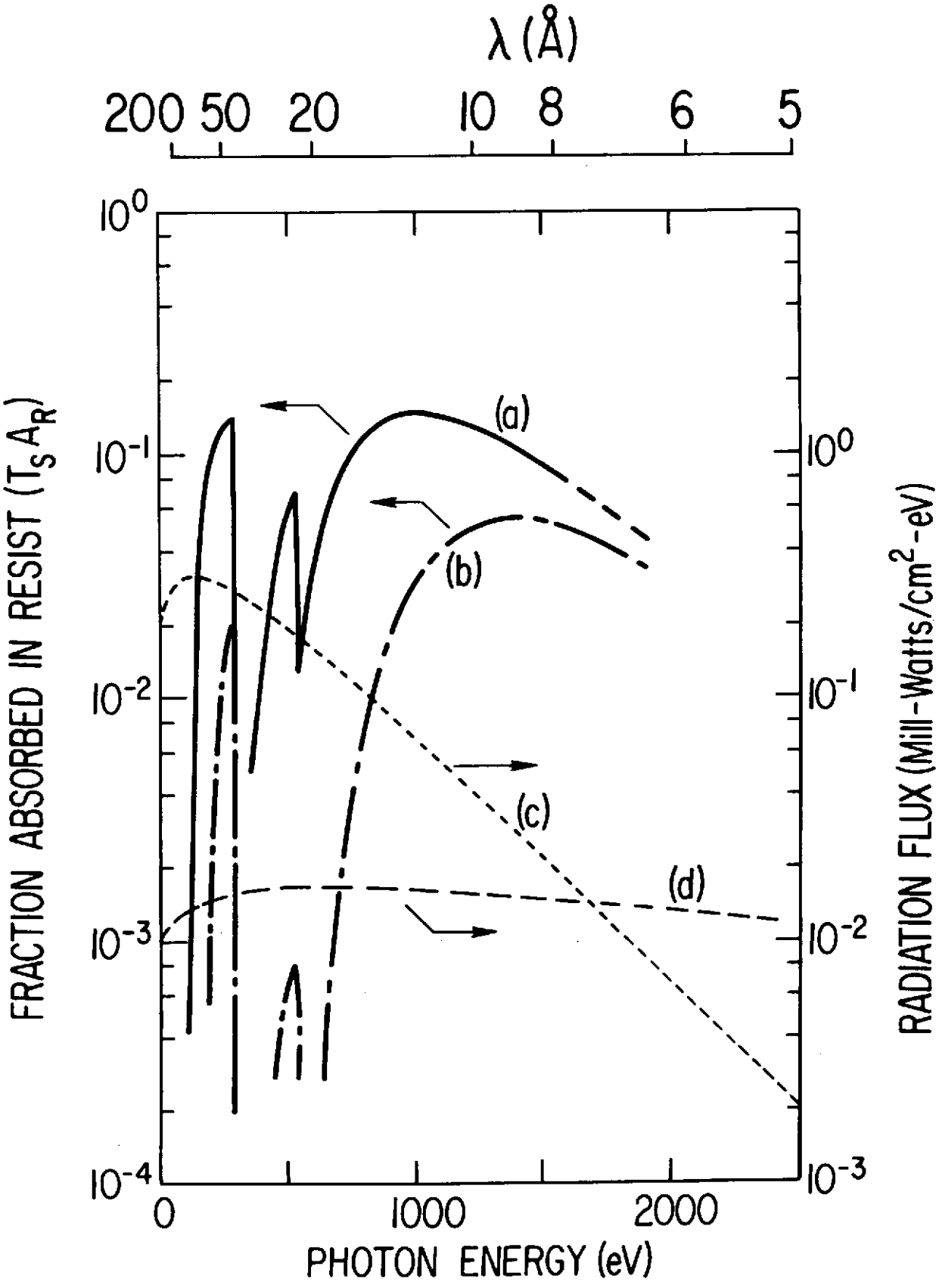
λ (Å)
200 50 20 10 8 6 5
10^0
10^{-1}
10^{-2}
10^{-3}
10^{-4}
(a)
(b)
(c)
(d)
FRACTION ABSORBED IN RESIST ($T_S A_R$)
RADIATION FLUX (Mill-Watts/cm^2-eV)
0
1000
2000
PHOTON ENERGY (eV)

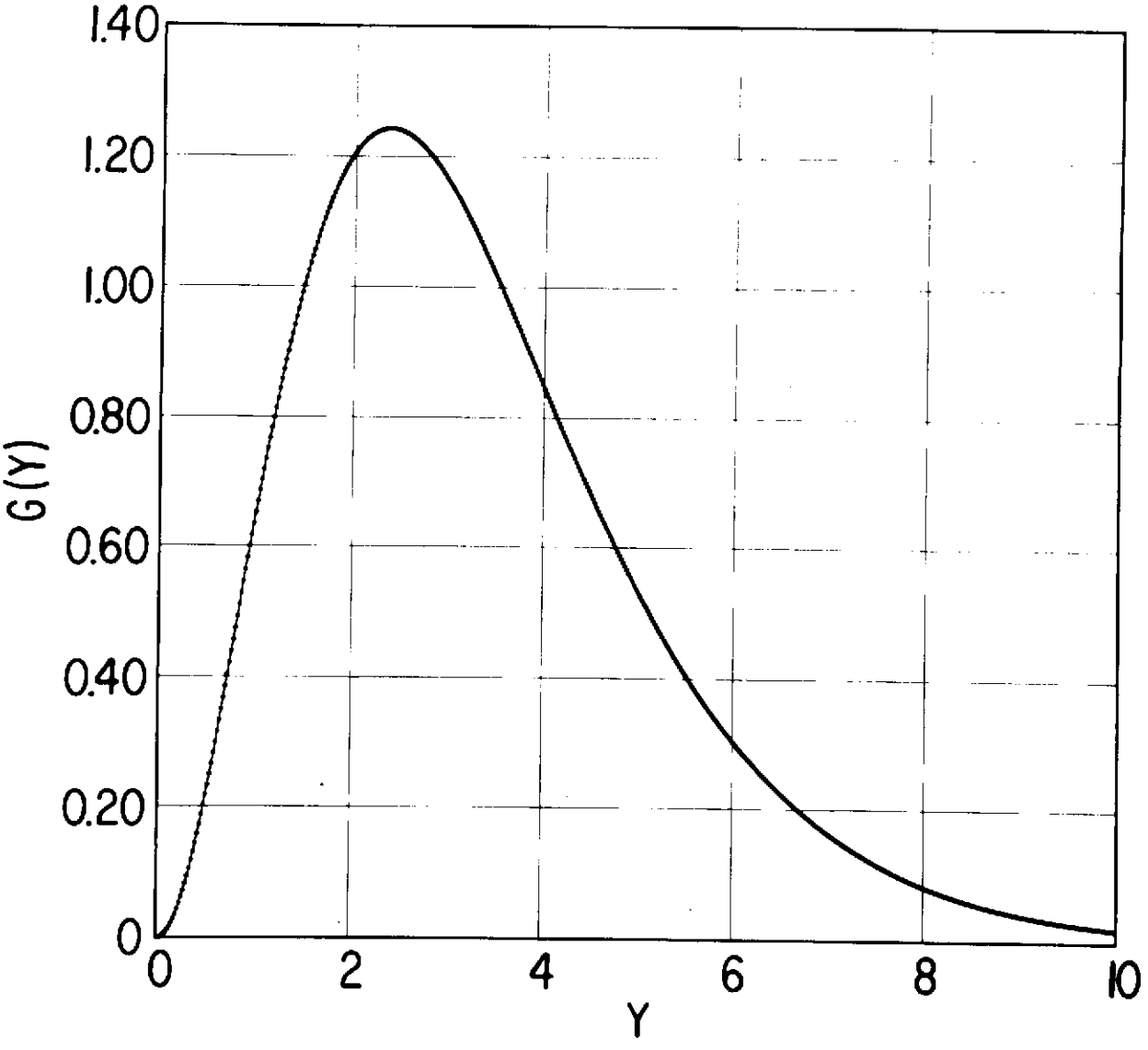
1.40
1.20
1.00
0.80
0.60
0.40
0.20
0
G(Y)
0
2
4
6
8
10
Y